

1 **Title: Evidence of Matuyama-Brunhes transition in the cave sediment in Central Europe**

2 **Hakan Ucar^{a*}, Gunther Kletetschka^{a,b,c}, Jaroslav Kadlec^d**

3 ^aFaculty of Science, Charles University, Prague, Czech Republic, ^bThe Czech Academy of
4 Sciences, Institute of Geology, Czech Republic ^cGeophysical Institute, University of Alaska
5 Fairbanks, AK, USA, ^dInstitute of Geophysics, Czech Academy of Sciences, Czech Republic.

6 *Corresponding author: ucarh@natur.cuni.cz

7 Co-author's emails: gunther.kletetschka@natur.cuni.cz; kadlec@ig.cas.cz

8 **Key Points**

- 9 • Paleomagnetic data shows Matuyama-Brunhes record in Central Europe cave
10 sediment.
- 11 • VGP data from caves can be used to date the Central European paleomagnetic record.
- 12 • Supporting data shows relationship between magnetic reversal and meteorite impact.

13 **Plain Language Summary**

14 The Earth has a significant property which is its magnetic field and rocks acquire a primary
15 magnetization in the Earth's magnetic field direction during their formation. There are
16 changes in this natural geomagnetic field throughout the Earth's history. One of these changes
17 is called magnetic reversal that magnetic North and South pole switches. Sediments recorded
18 Matuyama-Brunhes magnetic reversal which occurred 781 kyr ago. Investigation of the
19 reversals is possible by paleomagnetic methods which is a tool to understand the Earth's
20 magnetic field and its origin. Also there is a relationship between the reversals and meteorite
21 impacts which may be the trigger of these events. This new data from cave sediments show a
22 detailed paleomagnetic investigation of the reversal and a discussion of meteorite impact
23 hypothesis.

24

25

26 **Abstract**

27 In this study, we identified the Matuyama-Brunhes magnetic reversal recorded in cave
28 sediments in Central Europe, Czech Republic. We collected discrete samples from the
29 homogeneous sedimentary profile in the Za Hajovnou cave located in the eastern part of the
30 Czech Republic. Novel use of characteristic remanent magnetization (ChRM) directions and
31 VGP path of the data revealed Matuyama-Brunhes transition boundary within 5 cm of the Za
32 Hajovnou cave sediment. This result revealed a new more detailed behavior of the polarity
33 transition from the central European location. Migration of the paleopole between east of
34 Africa and west of North America is a significant marker in terms of the central European
35 paleomagnetic record. Also we estimated the sedimentation rate of the cave. In addition, we
36 discussed our results with a supporting data associated with tektites in the light of a new
37 hypothesis that a meteorite impact could be a reason of Matuyama-Brunhes reversal.

38 **Keywords:** Matuyama-Brunhes, paleomagnetism, magnetic reversal, cave, sediments,
39 meteorite impact

40 **1. Introduction**

41 Matuyama-Brunhes magnetic reversal occurred approximately 781 kyr ago (Lourens et al.,
42 2004). Studies in recent years (Channel et al., 2010; Giaccio et al., 2013; Jin and Liu, 2011;
43 Kitaba et al., 2013; Liu et al., 2016; Okada et al., 2017; Pares et al., 2016; Sagnotti et al.,
44 2010, 2014; Suganuma et al., 2010; Valet et al., 2014; Bella et al., 2019) have shown that this
45 event is well recorded by respective sediments that had sufficient sedimentation rate and
46 could be analyzed, in detail, by paleomagnetism.

47 Sediments acquire remanent magnetization during their deposition. The alignment of
48 ferromagnetic grains occurs in the direction of the earth's magnetic field and acquisition of
49 primary magnetization due to this sedimentation process is called depositional or detrital
50 remanent magnetization (DRM) (Gubbins and Herrero, 2017). Remanent magnetization

51 protected by energy barriers can last over geologic time scales. Nevertheless, due to thermal
52 and/or chemical processes such as reheating, oxidation and formation of iron hydroxides
53 during time, barriers may be overcome, the magnetic domains change their arrangement and
54 rocks can acquire secondary magnetizations. The new secondary magnetization has an
55 orientation in the direction of the Earth's field. Then rocks can acquire a viscous
56 magnetization (VRM) long time after their formation due to an exposure to geomagnetic field.
57 VRM contributes to a noise in paleomagnetic data (Lanza and Meloni, 2005; Butler, 1997).
58 Lock-in-depth affects the nature of the paleomagnetic recording process in sediments. It is
59 defined as the depth at which the remanent magnetization is stabilized. Lithology, grain-size
60 distribution of the sediment matrix, sedimentation rate and bioturbation, all have influence on
61 the position of the lock-in-depth in the sediments (Sagnotti et al., 2005; Bleil and von
62 Dobeneck, 1999). When assuming the steady sedimentation rate, the result of lock-in-depth
63 stabilization is younger magnetization than the sediment itself by an amount of time required
64 to accumulate sediment layer of thickness that equal to the lock-in-depth. For example, if the
65 sediment has accumulation speed 1 mm per 1000 years, and lock-in-depth is 10 mm, the
66 magnetization age is 10 000 years younger than the sediment itself (Sagnotti et al., 2005).
67 Kadlec et al. (2005, 2014) reported that the Central European cave (local name "Za
68 Hájovnou"), in the Moravia region of the Czech Republic, has a potential record of
69 Matuyama-Brunhes transition. Here we obtained a new paleomagnetic dataset from three
70 vertical sediment profiles found in this cave.

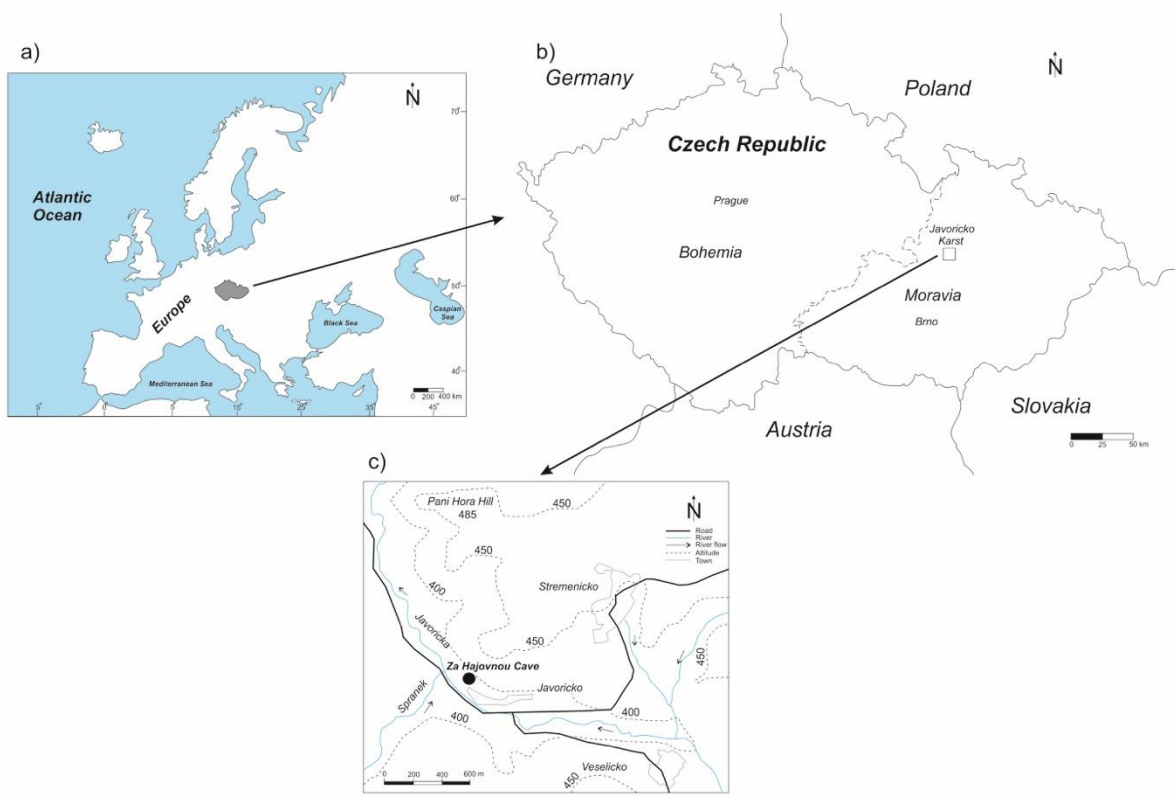
71 *1.1 Geology and Sampling*

72 The Za Hájovnou Cave (49° 40' N, 16° 55' E) is a former sinkhole located in Javoricko Karst,
73 Moravia Region of the Czech Republic (Lundberg et al., 2014; Musil, 2014) (Figure 1). The
74 Javoricko Karst is formed by light-grey-coloured massive Devonian limestone that overlies
75 Pre-Cambrian phyllite (Lundberg et al., 2014; Musil, 2014). Spranek and Javoricka are two

76 rivers that flow through the Jarovicko karst. While Za Hájovnou Cave is situated on the north-
77 western bank of the Javoříčka river on the southern slope of a Pani Hora hill (Lundberg et al.,
78 2014; Musil, 2014; Zak et al., 2018;), both Spranek and Javoricka watershed may have
79 contributed to the sediment development in this cave (Figure 1).

80 The Za Hajovnou cave is approximately 500 m long system (Babek et al., 2015; Musil, 2005).
81 The cave's corridors were expored previously in a total length of ~200 m (Musil, 2014)
82 (Figure 2). The cave currently consists of two main parallel corridors with slightly different
83 sedimentological record (Musil et al., 2014); the first corridor (local name is "Excavated
84 Corridor") used to be sinkhole entrance) and the other corridor (local name is "Birthday
85 Corridor") has separate entrance and is connected with the Excavated Corridor by the
86 Connecting Passage Corridor (Figure 2). Sediments from the Excavated Corridor continue to
87 Birthday Corridor and partially filled the Connecting Passage Corridor (Musil et al., 2014)
88 (Figure 2).

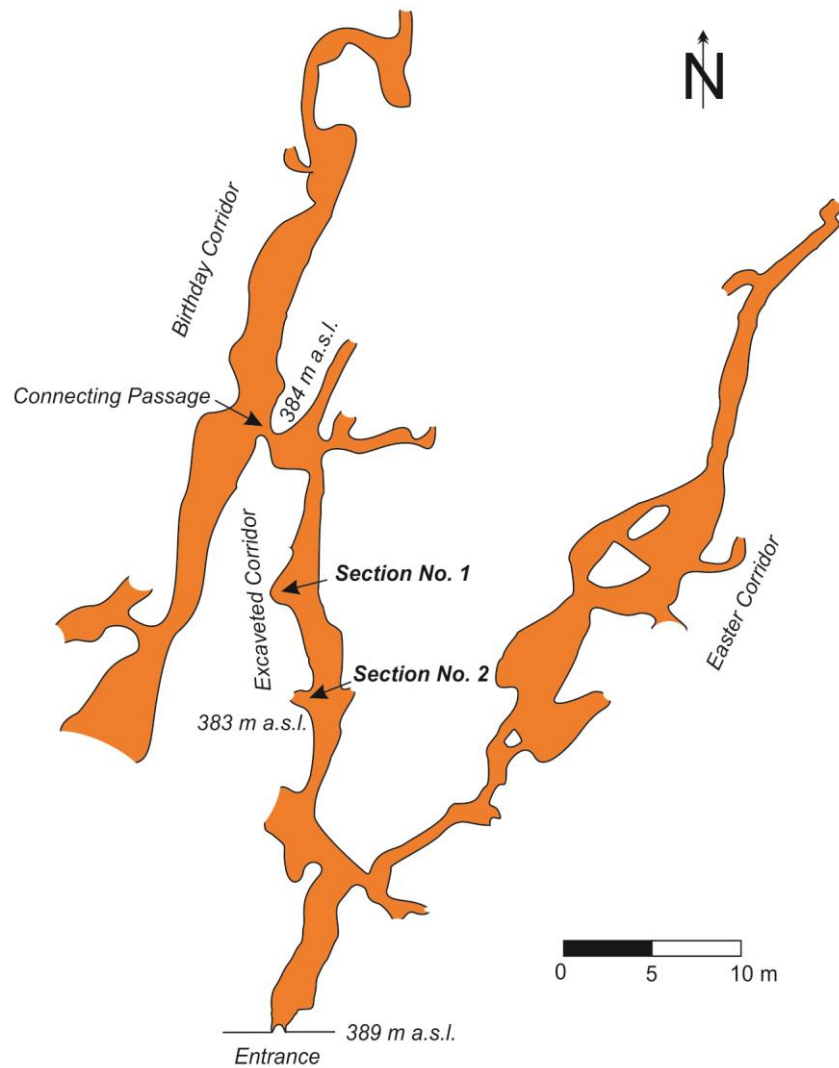
89



90

91 **Figure 1:** Location of the study area in a) Central Europe. Dashed lines in b) show more
 92 detailed placement different regions of the Czech Republic in relation to study area. Map in c)
 93 shows regional detail of the Za Hajovnou cave placement (modified after Lundberg et al.,
 94 2014; Musil, 2014).

95



96

97 **Figure 2:** Map of the Za Hajovnou cave (modified after Musil, 2014; Lundberg et al., 2014;
 98 Kadlec et al., 2014). Locations marked by “Section No. 1” and “Section No. 2” is discussed in
 99 the text (Kadlec et al., 2005, 2014). Map shows relation between Connecting Passage
 100 Corridor, Birthday Corridor, and Excavated Corridor (m a.s.l.: meter above sea level).

101

102 Upper sediments of the cave were dated by U/Th dating of flowstones to 118 ± 1 to 267 ± 3
 103 ka and by inferred Matuyama-Brunhes boundary in Section No. 1 (Figure 3) (Musil, 2005;
 104 Kadlec et al., 2005, 2014; Lundberg et al., 2014; Babek et al 2015). The sedimentation in the
 105 cave corridors were active probably from the Early Pleistocene until the beginning of the

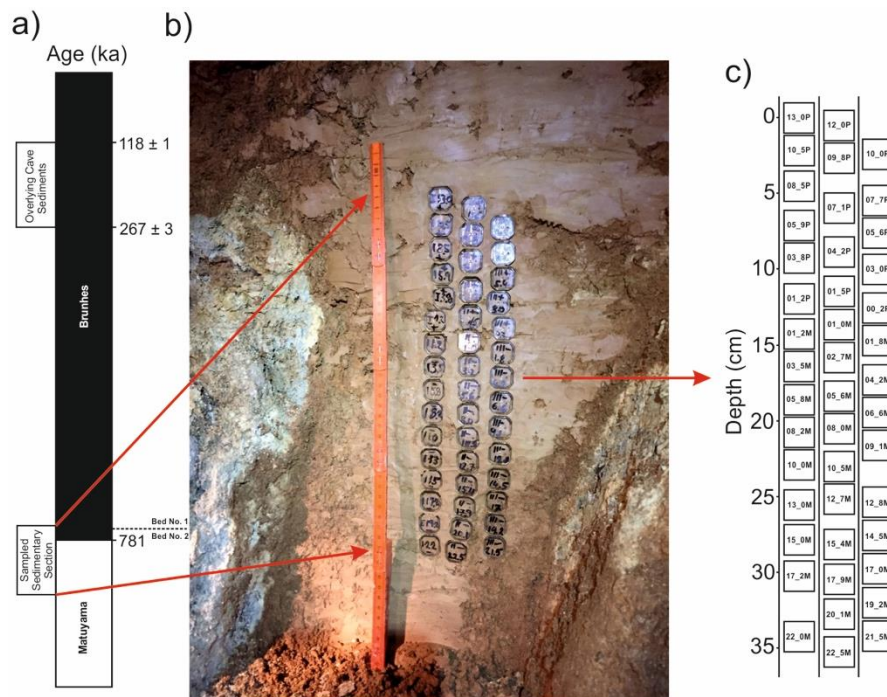
106 Middle Pleistocene. The sediment then consists of Pleistocene glacial time in north-western
107 Europe called Cromerian Interglacials complex (Muller, 1992), MIS19 (marine isotope stage)
108 which is interglacial period ~780 ka (Pol et al., 2019) and Matuyama-Brunhes reversal
109 (Kadlec et al. 2005, 2014; Musil et al., 2014; Musil, 2014; Zak et al., 2018; Lundberg et al.,
110 2014).

111 The Matuyama-Brunhes boundary (781 ka) was suggested in the upper part of the backwater
112 fine sediments, deposited from suspension in the flooded cave. These sediments underlay the
113 mostly non-fluvial deposits which entered the cave through a steep passage and filled the
114 Connecting Passage Corridor. (Kadlec et al., 2014; Lundberg et al., 2014; Musil et al., 2014).

115 Sedimentary sections retrieved in the Za Hajovnou cave by Kadlec et al. (2005, 2014) were
116 composed of two parts. The first part (Section No. 1, in Figure 2) was situated in the
117 Excavated Corridor about 28 m from the cave entrance (Kadlec et al., 2005) (Figure 2). It was
118 interpreted to contain the magnetic transition from a reversed to a normal polarity and inferred
119 from the age dates of the overlying non-fluvial sediments, that it could be the Matuyama-
120 Brunhes reversal (Kadlec et al., 2005). The second sedimentary section (Section No. 2)
121 partially overlapped the Section No. 1, and was located in the Excavated Corridor (Kadlec et
122 al., 2014) (Figure 2). Kadlec et al. (2014) indicated that this section had sediment with just
123 reversed polarity except upper part of the sediment where the magnetization was difficult to
124 interpret because the sediments had weak magnetization for which the sensitivity of the Agico
125 JR-6A spinner magnetometer was insufficient. Section No. 2 underlies the Section No. 1 and
126 contained older backwater sediment with reversed magnetic polarity (age > 781 ka, (Kadlec et
127 al., 2014)).

128 The difficulties in interpretation of the primary study by Kadlec et al. (2014) was the
129 motivation for the presented research. Here we collected 44 oriented discrete sedimentary

130 samples from the Excavated Corridor near the upper backwater sedimentary Section No. 1
131 (Figure 2, 3).



132
133 **Figure 3:** a) Age diagram of Za Hajovnou cave (dashed lines show the boundary between
134 Bed No. 1 and 2 b) Sampled sedimentary Section No. 1 and c) discrete samples (numbers
135 show the sample name).

136 137 2. Materials and Methods

138 2.1. Preparation of the Samples

139 The samples were placed in plastic boxes (2x2x2 cm; 8cc) for paleomagnetism studies. The
140 thickness of the sampled part of the sedimentary section was 35.1 cm. Lithology of the
141 sampled sedimentary section; The upper backwater fine sediment part was brown clayey silt
142 with white angular clasts of weathered limestone and bone fragments (Bed No. 1) (Kadlec et
143 al., 2014). Lower part of the section consisted of the brown silty clay without white clasts
144 (Bed No. 2) which is presented in Figure 3 (Kadlec et al., 2014).

145 2.2. Demagnetization Measurements

146 To clean the secondary magnetizations from the sedimentary samples, we applied a stepwise
147 alternative field (AF) demagnetization method in Pruhonice Paleomagnetism Laboratory of
148 Czech Academy of Sciences. This method was carried out using a 2G Enterprises Cryogenic
149 Magnetometer on 44 samples divided into 3 different sequences. The first sequence was 17
150 samples (13_0P, 10_5P, 09_8P, 08_5P, 05_9P, 03_8P, 01_2P, 01_2M, 03_5M, 05_8M,
151 08_2M, 10_0M, 13_0M, 15_0M, 17_2M, 19_2M, 22_0M) where we demagnetized at 1 mT
152 intervals between 0-49 mT and 10 mT intervals between 50-100 mT. The second sequence
153 was 14 samples (12_0P, 07_1P, 04_2P, 01_5P, 01_0M, 02_7M, 05_6M, 08_0M, 10_5M,
154 12_7M, 15_4M, 17_9M, 20_1M, 22_5M) where we demagnetized at 2 mT intervals between
155 0-48 mT and 10 mT intervals between 50-100 mT. The third sequence was 13 samples
156 (10_0P, 07_7M, 05_6P, 03_0P, 00_2P, 01_8M, 04_2M, 06_2M, 09_1M, 12_8M, 14_5M,
157 17_0M, 21_5M) and we demagnetized at 0.5 mT intervals between 0-39.5 mT and 10 mT
158 intervals between 40-100 mT. Demagnetization data was interpreted by using Remasoft
159 software which was written by Agico Company (Chadima and Hroudá, 2009).

160 Characteristic remanent magnetization (ChRM) directions and maximum angular deviation
161 (MAD) values were determined from principal component analysis (PCA) (Kirschvink 1980)
162 on Zijderveld diagram (Zijderveld, 1967). Virtual geomagnetic pole's (VGP's) latitudes and
163 longitudes were calculated using PMGSC software by Randy Enkin. Table 1 shows the data
164 of alternative field demagnetization for each individual sample. Two examples of alternative
165 field demagnetization method for Matuyama and Brunhes sections of the samples with
166 changes of declination, inclination angles and remanent magnetization intensity step by step
167 are given in Figure 4. Rest of the samples are in the supplementary table S1 and table S2
168 containing supplementary Figures. Maximum angular deviation (MAD) changes of this study
169 and comparisons with previous studies (Okada et al., 2017; Sagnotti et al., 2014) are shown in
170 Figure 5.

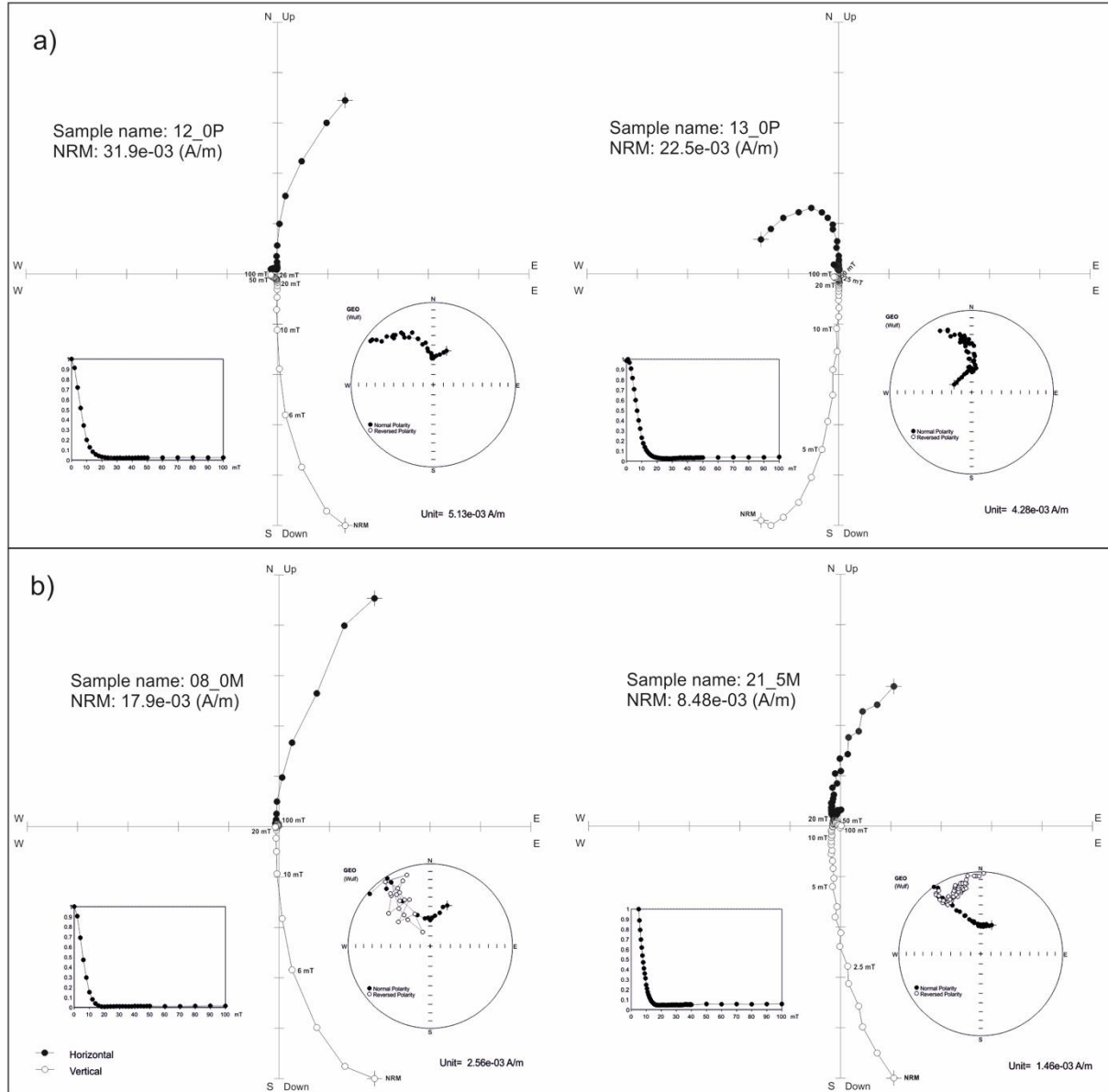
171 **Table 1:** Alternative field demagnetization, virtual geomagnetic pole (VGP) data and
 172 Matuyama-Brunhes magnetic reversal scale for this study. Minus (-) values for virtual
 173 geomagnetic pole (VGP) latitudes and longitudes indicate southern and western hemisphere.
 174 MAD: maximum angular deviation, ϕ_p : VGP latitude, λ_p : VGP longitude.

Sample Name	Depth (cm)	Dec ^(o)	Inc ^(o)	Intensity (A/m)	MAD ^(o)	ϕ_p (N°/S°)	λ_p (E°/W°)	
13_0P	0	369.2	65.9	7.56E-04	0.4	83.8	114.5	Brunhes
12_0P	-1	356.1	58.5	1.06E-03	1.8	79.4	-146.7	
10.5P	-2.5	379.7	37.8	8.03E-04	1.4	57.8	160.5	
10_0P	-3	407.1	44.3	7.96E-04	1.2	47	121.8	
09_8P	-3.2	401.1	33	1.04E-03	1	44.5	135.4	
08_5P	-4.5	378.5	43.2	7.02E-04	1.6	61.8	159.2	
07_7P	-5.3	378.7	25.2	7.47E-04	1.4	50.7	167.1	
07_1P	-5.9	356.1	37.3	9.54E-04	1.4	61.3	-155.8	
05_9P	-7.1	342.5	57.7	4.15E-04	1.4	73.3	-108.3	Transition
05_6P	-7.4	369.1	30.4	4.48E-04	1.1	56.1	-179.3	
04_2P	-8.8	338.7	2.1	1.01E-03	3.8	38.3	-135.9	
03_8P	-9.2	308.2	-8.4	7.45E-04	2.3	-20.2	73.2	
03_0P	-10	327.2	-32.7	1.26E-03	0.7	-16.8	49.1	
01_5P	-11.5	339.3	-15.8	6.87E-04	5.3	-29.8	40.3	
01_2P	-11.8	338.1	3.7	6.12E-04	2.6	38.9	-134.8	
00_2P	-12.8	345.3	-38.7	7.03E-04	1.3	-17.6	30.9	
01_0M	-13.6	369.6	-6.3	8.70E-04	1.4	-36.8	4.5	Matuyama
01_2M	-13.8	371.8	-21.3	5.04E-04	3.8	-28.7	3.3	

01_8M	-14.4	315.8	-49.2	1.55E-03	1.2	-1.3	53.7
02_7M	-15.3	320.5	-22.8	8.30E-04	4.2	-19.6	57.9
03_5M	-16.1	341.7	-33.3	5.45E-04	0.6	-20.5	35.1
04_2M	-16.8	305.2	-40.3	7.78E-04	1.1	-2.8	65.4
05_6M	-18.2	305.9	-32.6	5.18E-04	1.2	-7.6	67.7
05_8M	-18.4	362.3	-61	1.06E-03	1	-1.5	-165.2
06_6M	-19.2	282.8	-65.3	3.19E-04	3.5	-27.5	-165.4
08_0M	-20.6	320.1	-40.3	1.25E-04	5.4	-9.4	53.3
08_2M	-20.8	335.3	-31.6	1.37E-03	0.3	-20	41.7
09_1M	-21.7	357.1	-58.1	1.40E-04	4.2	-1.8	18.8
10_0M	-22.6	352.5	-66.2	1.27E-03	1.5	-8.2	-158.4
10_5M	-23.1	393.7	-88.7	1.72E-03	1.4	-47.2	-165.6
12_7M	-25.3	102.8	-83.7	8.05E-04	3	-50.6	177.2
12_8M	-25.4	230.5	-72.3	8.44E-04	1.6	-59.6	-108.3
13_0M	-25.6	299.2	-56.6	1.04E-03	0.5	-11.9	-118.2
14.5M	-27.1	238	-68.7	9.90E-04	0.9	-54.2	-100.5
15_M	-27.6	312	-40.3	7.71E-04	2.5	-6	60
15_4M	-28	180.1	-89.3	8.56E-04	0.4	-50.8	-163.4
17_0M	-29.6	234.5	-79.1	9.03E-04	0.5	-57.6	-130.3
17_2M	-29.8	294.7	-60.7	2.11E-03	0.5	-16.9	-117.6
17_9M	-30.5	316.8	-82.8	1.56E-03	0.7	-38.3	-151.1
19_2M	-31.8	291.6	-87.8	4.43E-04	1.3	-47.5	-157.1
20_1M	-32.7	256.8	-72	1.24E-03	1.5	-45.9	-113.8
21_5M	-34.1	323.3	-23.4	3.91E-04	3.2	-20.5	55.1

22_0M	-34.6	250.8	-61.9	2.40E-03	0.3	-42.5	-94.3
22_5M	-35.1	143.3	-78.8	1.58E-03	0.4	-63.9	166.6

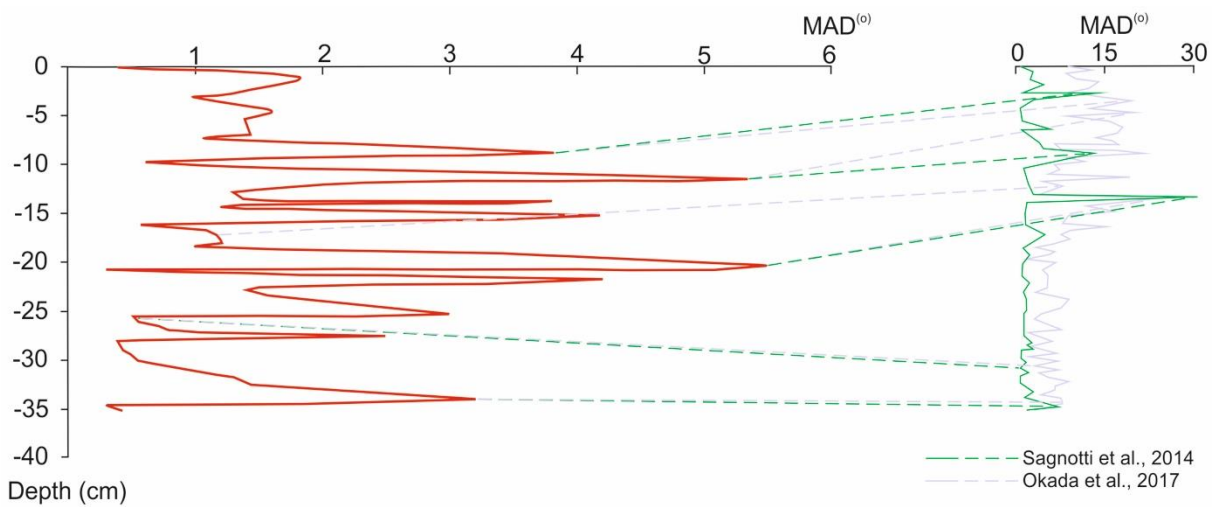
175



176

177 **Figure 4:** Changes of magnetization directions on Zijderveld diagram and Wulff stereonet
 178 during alternative field (AF) demagnetization method and demagnetization curve for typical
 179 samples (See Supplementary Figures (Table S2) for all other samples); a) normal polarity
 180 from Brunhes section (12_0P, 13_0P) and b) reversed polarity from Matuyama section
 181 (08_0M, 21_5M).

182
183



184

185 **Figure 5:** Comparison of Maximum angular deviation (MAD) changes from this data with
186 published studies. during Matuyama-Brunhes magnetic reversal. Maximum angular deviation
187 (MAD) values show error and confidence limit for this data during magnetic reversal, b:
188 Published MAD values for datasets from Okada et al. 2017; Sagnotti et al. 2014. Colourful
189 dashed lines connect sections published studies and this study where we see presentation of
190 similar variation.

191

192 3. Results

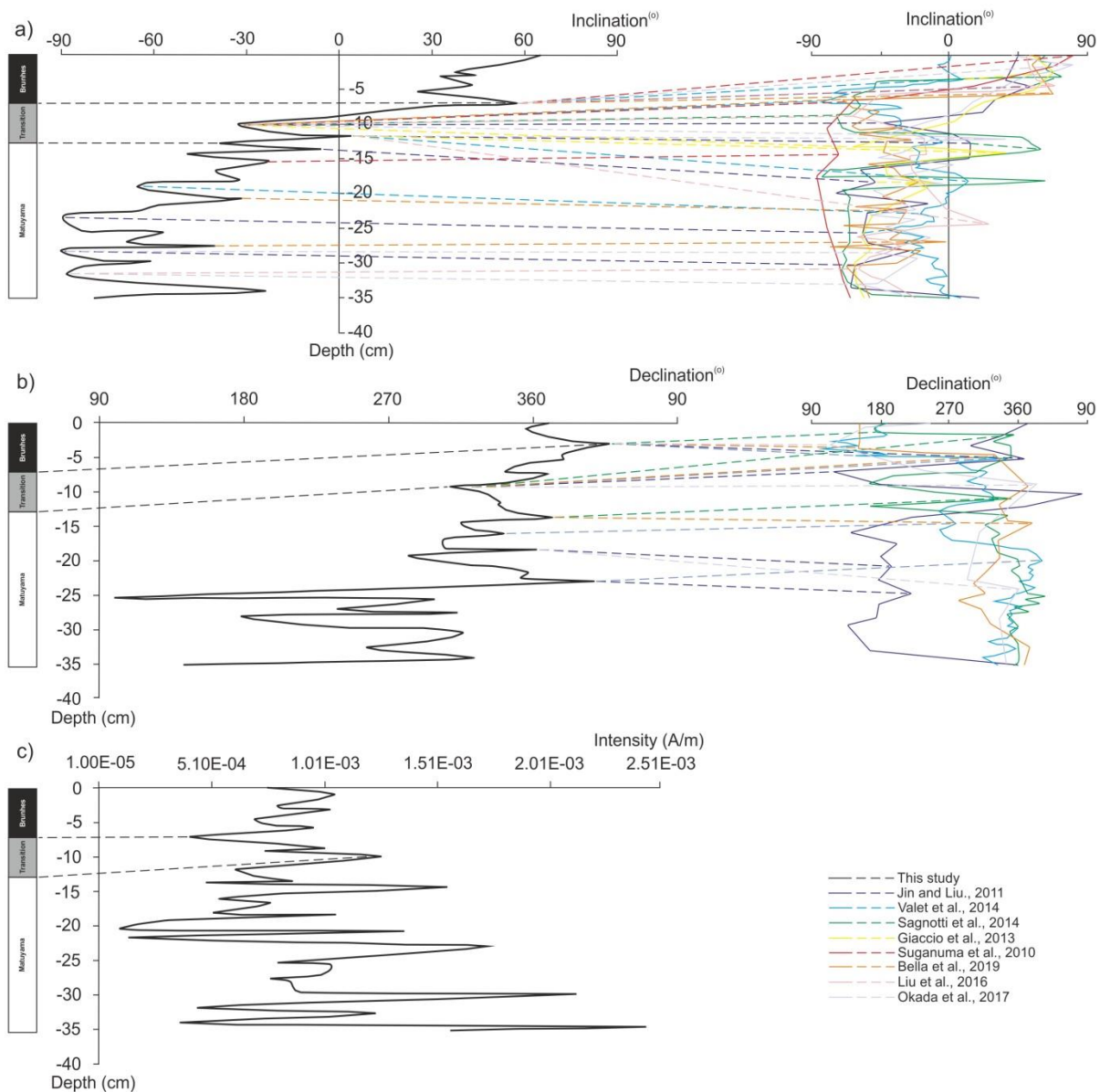
193 3.1. Paleomagnetic Results

194 Sedimentary samples were demagnetized generally up to 20 mT (for details see Table S2)
195 which removed the viscous remanent magnetization component causing change in the
196 direction of remanent magnetization during such demagnetization for most of the samples.
197 Intensity of the natural remanent magnetization (NRM) of the samples varies between 8.5-
198 34.1e-3 A/m. Median destructive field (MDF) values where samples lost half of its
199 magnetization range between 5-8 mT for the samples. NRM intensity and MDF values of the
200 samples are shown in supplementary figures (Table S3). Maximum angular deviation (MAD)

201 values for Matuyama and Brunhes sections are between 0.3° - 5.4° (Figure 5). These values for
202 transition section are between 0.7° - 5.3° which is relatively reliable for detection of the
203 migration of the paleomagnetic vector from a reversed to normal polarity (Figure 5).
204 Comparisons of MAD values with previous studies (Okada et al., 2017; Sagnotti et al., 2014)
205 shows the relative magnitude of fluctuations.

206 In this study, paleomagnetic data showed inclination values changing by approximately 90°
207 when measuring the sediment from 12.8 to 7.1 cm depth (Figure 6). This revealed the
208 transition nature of the Matuyama-Brunhes magnetic reversal in Za Hajovnou cave. Below
209 this depth, there is a Matuyama section which has inclination fluctuations between -6.3° - 88.7°
210 (Figure 6). Inclination angle changes between 33° - 65.9° for Brunhes section above transition
211 (Figure 6). Also, transition from reversed to normal polarity can be seen in declination data
212 with similar depth (Figure 6). Despite the fluctuations, magnetic intensity values which can
213 depend on the concentration variation of magnetic carriers of every individual sample, were
214 decreasing for the Matuyama section from the bottom to the transition (Figure 6). After the
215 transition from reversed to normal polarity, these values kept increasing which can be seen in
216 Brunhes section between 7.1-0 cm depth (Figure 6). Figure 6 shows the data in comparison
217 with other studies that consisted of various sediment types and locations around the world.
218 Depth of the data sets was normalized considering the transition zone and differences of
219 sedimentation rate for each study and is not given in Figure 5, 6. Even though, there are some
220 differences in absolute values, comparisons of this data set with other studies showed that
221 fluctuations and frequency of fluctuations in our data is consistent with other data sets and
222 serves as a supporting argument for Matuyama-Brunhes magnetic reversal in Za Hajovnou
223 cave (Figure 6).

224



225

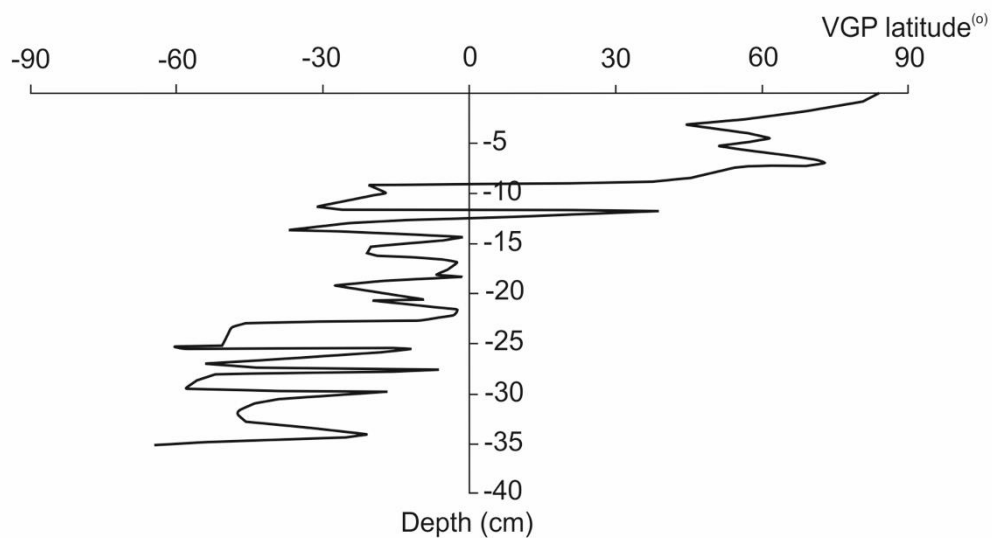
226 **Figure 6:** Comparisons of inclination and declination data with previous studies. As a result
 227 of alternative field demagnetization method, data shows a) Inclination, b) Declination and c)
 228 Magnetic intensity of the samples. Dashed lines in color connect sections published studies
 229 and this study where we see presentation of similar variation.

230

231 3.2. VGP's and Pole Migration

232 Virtual geomagnetic pole (VGP) shows the position of the geomagnetic paleopole (Lanza and
 233 Meloni, 2006). Virtual geomagnetic pole's (VGP) latitudes from this data set show fluctuations

234 in Matuyama section (Figure 7). These values indicate 90° change from Matuyama to
235 Brunhes transition as a result of pole migration (Figure 7). In addition, we plotted VGP path
236 for Matuyama, Brunhes and transition sections using VGP latitudes and longitudes based on
237 characteristic remanent magnetization (ChRM) directions detected in our samples (Figure 8).
238 VGP locations for Matuyama section is in the southern hemisphere (Figure 8). During the
239 transition from reversed to normal polarity, magnetic pole migrates from southern to northern
240 hemisphere (Figure 8). After the geomagnetic transition, paleopoles fluctuate around
241 geographic north pole (Figure 8). This VGP path of pole migration during the transition from
242 the southern to northern hemisphere compares well with the Matuyama-Brunhes transition
243 found by Okada et al. (2017) recorded in marine sediments near Japan (Figure 8).
244



245
246 **Figure 7:** Virtual geomagnetic pole (VGP) latitudes for this study.
247



248

249 **Figure 8:** a) Virtual geomagnetic pole (VGP) path of this study b) VGP path of transition
 250 section from Okada et al. 2017 (dashed lines show similarities between two study).

251

252 3.3. Sedimentation Rate

253 Sedimentation rate of the sediment from this study in the Za Hajovnou cave is not known. We
 254 compared the thickness of transition section of our study (cm) with the thickness of transition
 255 section of other studies (cm) and estimated the sedimentation rate. Let n be the ratio between

256 the two data sets which shows how thick or thin the transition section of previous study
 257 compared to our study (Equation 1.1, 1.2). This, we can estimate the sedimentation rate of Za
 258 Hajovnou (Equation 1.2). In equations, tso is the transition section thickness from our study
 259 (in cm), tsp is transition section thickness of published study (in cm), srp is sedimentation rate
 260 of published study (in cm/kyr), sro is sedimentation rate of our study (in cm/kyr).

261 Equations;

$$tso (cm) \times n = tsp (cm) \tag{1.1}$$

$$srp (cm/kyr) / n = sro (cm/kyr) \tag{1.2}$$

262

263 Then, Za Hajovnou sedimentation rate ranges between 0.07-1.40 cm/kyr. Dropping the
 264 highest (1.41 cm/kyr) and lowest (0.066 cm/kyr) values gives rate between (0.2 cm/kyr – 1.0
 265 cm/kyr) Sedimentation rate estimates are shown in Table 2 compared with other studies.

266

267 **Table 2:** Sedimentation rate estimations for Za Hajovnou from previous studies. *:
 268 Sedimentation rate estimation for Za Hajovnou.

Reference	Sedimentation Rate	Sedimentation Rate*
Jin and Liu. (2011)	15 cm/kyr	0.6 cm/kyr 270
Okada et al. (2017)	61 cm/kyr	0.91 cm/kyr271
Sagnotti et al. (2010)	61 cm/kyr	0.6 cm/kyr 272
Giaccio et al. (2013)	26 cm/kyr	1 cm/kyr 273
Sagnotti et al. (2014)	0.0224 cm/kyr	0.235 cm/kyr274
Suganuma et al. (2010)	0.66 cm/kyr	0.23 cm/kyr275
Bella et al. (2019)	0.64 cm/kyr	1.41 cm/kyr276
Liu et al. (2016)	8.78 cm/kyr	0.066 cm/kyr277

278 **4. Discussion**

279 Our data indicate that Matuyama Brunhes transition boundary constitutes 5.7 cm, between
280 7.1-12.8 cm depth of the sampled sedimentary section, of the Za Hajovnou cave sediment.
281 Magnetic reversal is characterized by frequent fluctuations of inclination angle (Figure 6a)
282 and VGP latitude (Figure 7). Maximum angular deviation (MAD) values of this study are
283 within the error limit as seen in Figure 5. Similarities in comparisons of this data set with
284 other studies indicate that Za Hajovnou cave sediment dates to Matuyama-Brunhes magnetic
285 transition.

286 Because of low coercivity in most of the samples with demagnetization generally at 20 mT,
287 some large fluctuations in the data may be considered as instability of remanent
288 magnetization. This shows that minerals with low coercivity is responsible for the
289 magnetization of the cave sediments in our study. On the other hand, similar fluctuations
290 which are seen in previous studies (Figure 6) show reliability of the data.

291 Although the data in this study and Okada et al. 2017 belong to geographically different
292 locations and sediment types, this similarity during polar migration shows that the reversal
293 was a dipole transition, and non-dipole field component was less significant (Simon et al.
294 2019; Mochizuki et al. 2011; Oda et al., 2000).

295 Our estimate of the Za Hajovnou cave's sedimentation rate seems to be significantly lower
296 than the sediments from other studies (Jin and Liu., 2011; Okada et al., 2017; Sagnotti et al.,
297 2010; Sagnotti et al., 2014; Giaccio et al., 2013; Sugauma et al., 2010; Bella et al., 2019; Liu
298 et al., 2016). This is likely due to contrasting sediment types.

299 Analyzes of cave sediments by paleomagnetism carried out in different locations around the
300 earth such as in Western Europe (Pares et al., 2018), South Africa (Nami et al., 2016), South
301 America (Jaqueto et al., 2016), North America (Stock et al., 2005), Southern Europe (Pruner
302 et al., 2010), Eastern Asia (Morinaga et al., 1992) showed that cave sediments recorded

303 magnetic reversals. Morinaga et al. (1992) suggested low sedimentation rate for the Western
304 Japan cave sediments 1.6 cm/kyr which shows similar rate with our Central European cave
305 sediment estimation. King and Channel (1991) suggested that large "lock-in" depths are
306 associated with interparticle rigidity and strength, characteristic of clayey low accumulation
307 rate sediments (<1 cm/kyr) which results in delays of magnetic acquisition. This shows that
308 magnetic polarity reversal could have a large (25 kyr) apparent age offset between sediments
309 with high and very low accumulation rates (King and Channel, 1991).

310 Glass and Heezen (1967) claimed that a meteorite impact could result in a magnetic reversal.
311 Large meteorite impacts may provide the sufficient moment to the exterior of the outer core to
312 cause motion relative to the outer core. In this way, the angular difference disrupts the
313 convection and the position of the magnetic poles. Changing in the convection pattern would
314 affect the electric currents in the liquid core to have a new core convection with modified
315 Coriolis forces. In addition the inner core's angular momentum change due to the new core
316 convection dynamics, in respect to the mantle, would change the heat transfer in the inner
317 core and have an effect on dynamo reset. This process may cause variations in the currents
318 producing the earth's magnetic field and cause a geomagnetic reversal. In our study, the
319 inclination and VGP change which have an anomaly about 12 cm depth just before the
320 reversal (Figure 6, 7) could be a reason of a meteorite impact which was shown in a study in
321 Indonesia from marine sediments (Hyodo et al., 2011) by micro-tektite level formed due to
322 cosmic impacts. This can be supported with oscillations in VGP's latitude approximately at
323 the same depth (1.5 m) below the reversal in the study of Yamazaki and Oda (2001) in South
324 Atlantic. Both of the studies (Hyodo et al., 2001; Yamazaki and Oda, 2001) have very similar
325 sedimentation rates between 8-10 cm/kyr. The same anomaly can be seen in sediments from
326 other studies (Sagnotti et al., 2014; Giaccio et al., 2013; Valet et al., 2014; Jin and Liu, 2011;
327 Liu et al., 2016; Okada et al., 2017) (Figure 6). Migration of the pole during Matuyama

328 polarity is towards to South America (Figure 8) which may be caused by the angular
329 momentum and convection pattern change because of the northward directed meteorite impact
330 in Asia (Sieh et al., 2020).

331 **5. Conclusions**

332 We compared the paleomagnetic data from the cave sediments with published magnetic
333 reversal record and were able for the first time to use the detailed magnetic characteristic of
334 cave sediment and to infer the specific magnetic reversal (Matuyama-Brunhes). This is
335 possible due to nature of the magnetic reversal that we discovered. Note that the paleopole
336 was residing in the east of Africa and than quickly reappeared west of North America. We
337 consider this as an important marker signature for dating the central European paleomagnetic
338 record from this time period.

339 Additionally, we were able to design a new method for estimation of the accumulation rate of
340 the cave sediment in Za Hajovnou cave, which until now was not known. Also we provided
341 an evidence that a meteorite impact could be the cause of the Matuyama-Brunhes magnetic
342 reversal.

343 **Acknowledgements**

344 We thank Kristina Kdyrova for their help with sample preparation and measurements and
345 Pruhonice Paleomagnetism Laboratory for allowing to measure the cave sediment samples.
346 Support for GK came from the Czech Science Foundation 20-08294S, 20-00892L, Ministry
347 of Education, Youth and Sports LTAUSA 19141, and institutional support RVO 67985831.
348 Data will be uploaded to MagIC (<https://www2.earthref.org/MagIC>) upon acceptance. Data is
349 currently uploaded as Supporting Information.

350

351

352 **References**

- 353 Bábek, O., Bristenský, M., Precechtlová, G., Štípaněíková, P., Hellstrom, J.C., Drysdale,
354 R.N., 2015. Pleistocene speleothem fracturing in the foreland of Western Carpathians: a
355 case study from the seismically active eastern margin of the Bohemian Massif. *Geological*
356 *Quarterly*, 59 (3): 491–506. <https://doi.org/10.7306/gq.1225>
- 357 Bella, P., Bosák, P., Braucher, R., Pruner, P., Hercman, H., Minár, J., Veselský, M., Holec, J.
358 and Léanni, L., 2019. Multi-level Domica–Baradla cave system (Slovakia, Hungary):
359 Middle Pliocene–Pleistocene evolution and implications for the denudation chronology of
360 the Western Carpathians. *Geomorphology*, 327, pp.62-79. <https://doi.org/10.1016/j.geomor>
361 [ph.2018.10.002](https://doi.org/10.1016/j.geomor.2018.10.002)
- 362 Bleil, U. and Von Dobeneck, T., 1999. Geomagnetic events and relative paleointensity
363 records—clues to high-resolution paleomagnetic chronostratigraphies of Late Quaternary
364 marine sediments?. In *Use of proxies in paleoceanography*(pp. 635-654). Springer, Berlin,
365 Heidelberg.
- 366 Butler, R.F. and Butler, R.F., 1992. *Paleomagnetism: magnetic domains to geologic*
367 *terraces* (Vol. 319). Boston: Blackwell Scientific Publications.
- 368 Chadima, M. and Hroudá, F., 2009. Remasoft)Paleomagnetic data browser and analyzer for
369 Windows). Agico s.r.o.
- 370 Channell, J.E., Hodell, D.A., Singer, B.S. and Xuan, C., 2010. Reconciling astrochronological
371 and $^{40}\text{Ar}/^{39}\text{Ar}$ ages for the Matuyama-Brunhes boundary and late Matuyama
372 Chron. *Geochemistry, Geophysics, Geosystems*, 11(12). <https://doi.org/10.1029/2010GC00>
373 [3203](https://doi.org/10.1029/2010GC003203)
- 374 Giaccio, B., Castorina, F., Nomade, S., Scardia, G., Voltaggio, M. and Sagnotti, L., 2013.
375 Revised chronology of the Sulmona lacustrine succession, central Italy. *Journal of*
376 *Quaternary Science*, 28(6), pp.545-551. <https://doi.org/10.1002/jqs.2647>

377 Glass, B. and Heezen, B.C., 1967. Tektites and geomagnetic reversals. *Nature*, 214(5086),
378 p.372. <https://doi.org/10.1038/214372a0>

379 Gubbins, D. and Herrero-Bervera, E. eds., 2007. *Encyclopedia of geomagnetism and*
380 *paleomagnetism*. Springer Science & Business Media.

381 Hyodo, M., Matsu'ura, S., Kamishima, Y., Kondo, M., Takeshita, Y., Kitaba, I., Danhara, T.,
382 Aziz, F., Kurniawan, I. and Kumai, H., 2011. High-resolution record of the Matuyama–
383 Brunhes transition constrains the age of Javanese Homo erectus in the Sangiran dome,
384 Indonesia. *Proceedings of the National Academy of Sciences*, 108(49), pp.19563-19568.
385 <https://doi.org/10.1073/pnas.1113106108>

386 Jaqueto, P., Trindade, R.I., Hartmann, G.A., Novello, V.F., Cruz, F.W., Karmann, I., Strauss,
387 B.E. and Feinberg, J.M., 2016. Linking speleothem and soil magnetism in the Pau d'Alho
388 cave (central South America). *Journal of Geophysical Research: Solid Earth*, 121(10),
389 pp.7024-7039. <https://doi.org/10.1002/2016JB013541>

390 Jin, C. and Liu, Q., 2011. Revisiting the stratigraphic position of the Matuyama–Brunhes
391 geomagnetic polarity boundary in Chinese loess. *Palaeogeography, Palaeoclimatology,*
392 *Palaeoecology*, 299(1-2), pp.309-317. <https://doi.org/10.1016/j.palaeo.2010.11.011>

393 Kadlec, J., Chadima, M., Pruner, P. and Schnabl, P., 2005. Paleomagnetic dating of sediments
394 in the “Za Hájovnou” cave in Javoříčko - preliminary results. *Natural Studies of the*
395 *Museum of the Prostějov Region* , 8 , pp.75-82.

396 Kadlec, J., Čížková, K. and Šlechta, S., 2014. New updated results of paleomagnetic dating of
397 cave deposits exposed in the “Za Hájovnou” Cave, Javoříčko Karst. *Acta Musei Nationalis*
398 *Pragae, Ser. B, Historia Naturalis*, 70(1-2). <https://doi.org/10.14446/AMNP.2014.27>

399 King, J.W. and Channell, J.E., 1991. Sedimentary magnetism, environmental magnetism, and
400 magnetostratigraphy. *Reviews of Geophysics*, 29(S1), pp.358-370.

401 Kirschvink, J.L., 1980. The least-squares line and plane and the analysis of palaeomagnetic
402 data. *Geophysical Journal International*, 62(3), pp.699-718.

403 Kitaba, I., Hyodo, M., Katoh, S., Dettman, D.L. and Sato, H., 2013. Midlatitude cooling
404 caused by geomagnetic field minimum during polarity reversal. *Proceedings of the*
405 *National Academy of Sciences*, 110(4), pp.1215-1220. [https://doi.org/10.1073/pnas.](https://doi.org/10.1073/pnas.1213389110)
406 [1213389110](https://doi.org/10.1073/pnas.1213389110)

407 Lanza, R. and Meloni, A., 2006. *The Earth's magnetism* (Vol. 280). Springer-Verlag Berlin
408 Heidelberg.

409 Liu, J., Liu, Q., Zhang, X., Liu, J., Wu, Z., Mei, X., Shi, X. and Zhao, Q., 2016.
410 Magnetostratigraphy of a long Quaternary sediment core in the South Yellow
411 Sea. *Quaternary Science Reviews*, 144, pp.1-15. [https://doi.org/10.1016/j.quascirev.2016.](https://doi.org/10.1016/j.quascirev.2016.05.025)
412 [05.025](https://doi.org/10.1016/j.quascirev.2016.05.025)

413 Lourens, L. J., F. J. Hilgen, J. Laskar, N. J. Shackleton, and D. Wilson. 2004. The Neogene
414 period, in A Geologic Time Scale 2004, edited by F. M. Gradstein, J. G. Ogg, and A. G.
415 Smith, pp. 409–440, Cambridge Univ. Press, Cambridge, U. K.

416 Lundberg, J., Musil, R. and Sabol, M., 2014. Sedimentary history of Za Hájojnou cave
417 (Moravia, Czech Republic): a unique middle Pleistocene palaeontological site. *Quaternary*
418 *International*, 339, pp.11-24. <https://doi.org/10.1016/j.quaint.2013.04.006>

419 Mochizuki, N., Oda, H., Ishizuka, O., Yamazaki, T. and Tsunakawa, H., 2011. Paleointensity
420 variation across the Matuyama-Brunhes polarity transition: Observations from lavas at
421 Punaruu Valley, Tahiti. *Journal of Geophysical Research: Solid Earth*, 116(B6).
422 <https://doi.org/10.1029/2010JB008093>

423 Morinaga, H., Horie, I. and Yaskawa, K., 1992. A geomagnetic reversal recorded in a
424 stalagmite collected in western Japan. *Journal of geomagnetism and geoelectricity*, 44(8),
425 pp.661-675. <https://doi.org/10.5636/jgg.44.661>

426 Muller, H., 1992. Climate changes during and at the end of the interglacials of the Cromerian
427 Complex. In *Start of a Glacial*(pp. 51-69). Springer, Berlin, Heidelberg.

428 Musil, R., 2005. Jeskyně Za Hájovnou, vyjímečná lokalita Javoříčského krasu. Musil, R,
429 pp.9-42.

430 Musil, R., 2014. The Unique Record Of Za Hájovnou Cave. *Acta Musei Nationalis Pragae*,
431 *Series B-Historia Naturalis*, 70. <https://doi.org/10.14446/AMNP.2014.7>

432 Musil, R., Sabol, M., Ivanov, M. And Doláková, N., 2014. Middle Pleistocene Stratigraphy
433 Of The Deposits In Za Hájovnou Cave (Javoříčko Karst, Northern Moravia, Czech
434 Republic). *Acta Musei Nationalis Pragae, Series B-Historia Naturalis*, 70.
435 <https://doi.org/10.14446/AMNP.2014.107>

436 Nami, H.G., de la Pefia, P., Vásquez, C.A., Feathers, J. and Wurz, S., 2016. Palaeomagnetic
437 results and new dates of sedimentary deposits from Klasies River Cave 1, South
438 Africa. *South African Journal of Science*, 112(11-12), pp.1-12. [https://doi.org/10.17159/
439 sajs.2016/20160051](https://doi.org/10.17159/sajs.2016/20160051)

440 Oda, H., Shibuya, H. and Hsu, V., 2000. Palaeomagnetic records of the Brunhes/Matuyama
441 polarity transition from ODP Leg 124 (Celebes and Sulu seas). *Geophysical Journal
442 International*, 142(2), pp.319-338. <https://doi.org/10.1046/j.1365-246x.2000.00130.x>

443 Okada, M., Suganuma, Y., Haneda, Y. and Kazaoka, O., 2017. Paleomagnetic direction and
444 paleointensity variations during the Matuyama–Brunhes polarity transition from a marine
445 succession in the Chiba composite section of the Boso Peninsula, central Japan. *Earth,
446 Planets and Space*, 69(1), p.45. <https://doi.org/10.1186/s40623-017-0627-1>

447 Parés, J.M., Arnold, L., Duval, M., Demuro, M., Pérez-González, A., de Castro, J.B.,
448 Carbonell, E. and Arsuaga, J.L., 2013. Reassessing the age of Atapuerca-TD6 (Spain): new
449 paleomagnetic results. *Journal of Archaeological Science*, 40(12), pp.4586-4595.
450 <https://doi.org/10.1016/j.jas.2013.06.013>

451 Parés, J.M., Álvarez, C., Sier, M., Moreno, D., Duval, M., Woodhead, J.D., Ortega, A.I.,
452 Campaña, I., Rosell, J., de Castro, J.B. and Carbonell, E., 2018. Chronology of the cave
453 interior sediments at Gran Dolina archaeological site, Atapuerca (Spain). *Quaternary*
454 *Science Reviews*, 186, pp.1-16. <https://doi.org/10.1016/j.quascirev.2018.02.004>

455 Pol, K., Masson-Delmotte, V., Johnsen, S., Bigler, M., Cattani, O., Durand, G., Falourd, S.,
456 Jouzel, J., Minster, B., Parrenin, F. and Ritz, C., 2010. New MIS 19 EPICA Dome C high
457 resolution deuterium data: Hints for a problematic preservation of climate variability at
458 sub-millennial scale in the “oldest ice”. *Earth and planetary science letters*, 298(1-2),
459 pp.95-103. <https://doi.org/10.1016/j.epsl.2010.07.030>

460 Pruner, P., Hajna, N.Z., Mihevc, A., Bosák, P., Man, O., Schnabl, P. and Venhodová, D.,
461 2010. Magnetostratigraphy and fold tests from Račiška pečina and Pečina v Borštu caves
462 (Classical Karst, Slovenia). *Studia Geophysica et Geodaetica*, 54(1), pp.27-48.

463 Sagnotti, L., Budillon, F., Dinarès-Turell, J., Iorio, M. and Macrì, P., 2005. Evidence for a
464 variable paleomagnetic lock-in depth in the Holocene sequence from the Salerno Gulf
465 (Italy): Implications for “high-resolution” paleomagnetic dating. *Geochemistry,*
466 *Geophysics, Geosystems*, 6(11). <https://doi.org/10.1029/2005GC001043>

467 Sagnotti, L., Cascella, A., Ciaranfi, N., Macrì, P., Maiorano, P., Marino, M. and Taddeucci, J.,
468 2010. Rock magnetism and palaeomagnetism of the Montalbano Jonico section (Italy):
469 evidence for late diagenetic growth of greigite and implications for
470 magnetostratigraphy. *Geophysical Journal International*, 180(3), pp.1049-1066.
471 <https://doi.org/10.1111/j.1365-246X.2009.04480.x>

472 Sagnotti, L., Scardia, G., Giaccio, B., Liddicoat, J.C., Nomade, S., Renne, P.R. and Sprain,
473 C.J., 2014. Extremely rapid directional change during Matuyama-Brunhes geomagnetic
474 polarity reversal. *Geophysical Journal International*, 199(2), pp.1110-1124. [https://doi.org/](https://doi.org/10.1093/gji/ggu287)
475 [10.1093/gji/ggu287](https://doi.org/10.1093/gji/ggu287)

476 Sieh, K., Herrin, J., Jicha, B., Angel, D.S., Moore, J.D., Banerjee, P., Wiwegwin, W.,
477 Sihavong, V., Singer, B., Chualaowanich, T. and Charusiri, P., 2020. Australasian impact
478 crater buried under the Bolaven volcanic field, Southern Laos. *Proceedings of the National*
479 *Academy of Sciences*, 117(3), pp.1346-1353. <https://doi.org/10.1073/pnas.1904368116>

480 Simon, Q., Sugauma, Y., Okada, M., Haneda, Y. and ASTER Team, 2019. High-resolution
481 ¹⁰Be and paleomagnetic recording of the last polarity reversal in the Chiba composite
482 section: Age and dynamics of the Matuyama–Brunhes transition. *Earth and Planetary*
483 *Science Letters*, 519, pp.92-100. <https://doi.org/10.1016/j.epsl.2019.05.004>

484 Stock, G.M., Granger, D.E., Sasowsky, I.D., Anderson, R.S. and Finkel, R.C., 2005.
485 Comparison of U–Th, paleomagnetism, and cosmogenic burial methods for dating caves:
486 implications for landscape evolution studies. *Earth and Planetary Science Letters*, 236(1-
487 2), pp.388-403. <https://doi.org/10.1016/j.epsl.2005.04.024>

488 Sugauma, Y., Yokoyama, Y., Yamazaki, T., Kawamura, K., Horng, C.S. and Matsuzaki, H.,
489 2010. ¹⁰Be evidence for delayed acquisition of remanent magnetization in marine
490 sediments: Implication for a new age for the Matuyama–Brunhes boundary. *Earth and*
491 *Planetary Science Letters*, 296(3-4), pp.443-450. [https://doi.org/10.1016/j.epsl.2010.05.](https://doi.org/10.1016/j.epsl.2010.05.031)
492 [031](https://doi.org/10.1016/j.epsl.2010.05.031)

493 Valet, J.P., Bassinot, F., Bouilloux, A., Bourlès, D., Nomade, S., Guillou, V., Lopes, F.,
494 Thouveny, N. and Dewilde, F., 2014. Geomagnetic, cosmogenic and climatic changes
495 across the last geomagnetic reversal from Equatorial Indian Ocean sediments. *Earth and*
496 *Planetary Science Letters*, 397, pp.67-79. <https://doi.org/10.1016/j.epsl.2014.03.053>

497 Yamazaki, T. and Oda, H., 2001. A Brunhes–Matuyama polarity transition record from anoxic
498 sediments in the South Atlantic (Ocean Drilling Program Hole 1082C). *Earth, planets and*
499 *space*, 53(8), pp.817-827. <https://doi.org/10.1186/BF03351679>

- 500 Zak, K., Liptak, V., Orvosova, M., Filippi, M., Hercman, H. and Matouskova, S., 2018.
501 Cryogenic carbonates and cryogenic speleothem damage in the Za Hájovnou Cave
502 (Javoříčko Karst, Czech Republic). *Geological Quarterly*, 62(4), pp.829-839.
503 <https://doi.org/10.7306/gq.1441>
- 504 Zijderveld, J.D.A., 1967. AC demagnetization of rocks: Analysis of results, Methods in
505 Paleomagnetism DW Collinson, KM Creer, SK Runcorn, 254–286.

1 Dear JGR Earth Surface editors,

2

3 We are submitting the manuscript "Evidence of Matuyama-Brunhes Transition in the Cave
4 Sediment in Central Europe" by H. Ucar, G. Kletetschka and J. Kadlec representing 4
5 institutions with student as a first author. We are submitting this as an article with
6 Supplementary Information.

7 In the attached manuscript, we present paleomagnetic evidence of a cave sediment sequence
8 from the Central European cave Za Hajovnou in Czech Republic in support of the Matuyama-
9 Brunhes magnetic reversal.

10

11 We feel that this topic is of interest to JGR Earth Surface. Please consider this new manuscript
12 for publication.

13

14 This contribution is novel and significant for number of reasons, as follows:

15 • For the first time, we show detailed paleomagnetic analyses of the cave sediment
16 which was referred as the potential record of Matuyama-Brunhes reversal by previous studies.

17 • We identified the record of Matuyama-Brunhes magnetic reversal record in the cave
18 sediment by showing that the detail of pole transition matches with previous studies on
19 sediments from locations around the earth.

20 • We show that details of paleopole migration from the cave sediments can be used as a
21 practical marker for dating the central European paleomagnetic record from this time period.

22 • This is the first report of sedimentation rate in the Za Hajovnou cave sediment using a
23 novel method.

24 • We discussed the hypothesis about magnetic reversal and a meteorite impact in Asia
25 with supporting data.

26

27 **Author Contributions:**

28 Ucar Hakan (HU), Kletetschka Gunther (GK), Kadlec Jaroslav (JK)

29 HU and GK designed research and wrote the paper, JK contributed on the field work, gave
30 detailed information about the cave sediment and commented significantly.

31

32 Authors declare that they have no known conflict of interest with any person or financial
33 support.

34

35 We would like to suggest reviewers for this article;

36

37 1) James H. Wittke

38 Division of Geosciences, School of Earth and Sustainability, College of the Environment,
39 Forestry, and Natural Sciences, Northern Arizona University, Arizona, USA

40 E-mail: James.Wittke@nau.edu

41 Reason: He is a researcher who works on meteorite impacts.

42

43 2) Jiri Mizera

44 Nuclear Physics Institute of the Czech Academy of Sciences, Husinec, Czech Republic

45 E-mail: mizera@ujf.cas.cz

46 Reason: He is a researcher who works on tektites.

47

48 3) Toshitsugu Yamazaki

49 Department of Ocean Floor Geoscience, Atmosphere and Ocean Research Institute,
50 University of Tokyo, Tokyo, Japan

51 E-mail: yamazaki@aori.u-tokyo.ac.jp

52 Reason: We refer to his study on paleomagnetism.

53

54 4) Jean-Pierre Valet

55 Institut de Physique du Globe de Paris, Universite Paris Diderot, Paris, France

56 E-mail: valet@ipgp.fr

57 Reason: We refer to his study on paleomagnetism.

58

59

60 5) Pavel Bella

61 a) Department of Geography, Faculty of Education, Catholic University in Ružomberok,
62 Hrabovská cesta 1, 031 04 Ružomberok, Slovakia

63 b) State Nature Conservancy of the Slovak Republic, Slovak Caves Administration, Hodžova
64 11, 031 01 Liptovský Mikuláš, Slovakia

65 E-mail: pavel.bella@ssj.sk

66 Reason: We refer to his study on paleomagnetism in cave sediments.

67

68 Sincerely,

69 Hakan Ucar

1 Dear JGR Earth Surface editors,

2

3 We are submitting the manuscript “Evidence of Matuyama-Brunhes Transition in the Cave
4 Sediment in Central Europe” by H. Ucar, G. Kletetschka and J. Kadlec.

5

6 The “Highlights” of the manuscript is as follows:

- 7 • Paleomagnetic data shows Matuyama-Brunhes record in Central Europe cave
8 sediment.
- 9 • VGP data from caves can be used to date the Central European paleomagnetic record.
- 10 • Estimation shows sedimentation rate of Za Hajovnou cave sediment for the first time.
- 11 • Supporting data shows relationship between magnetic reversal and meteorite impact.

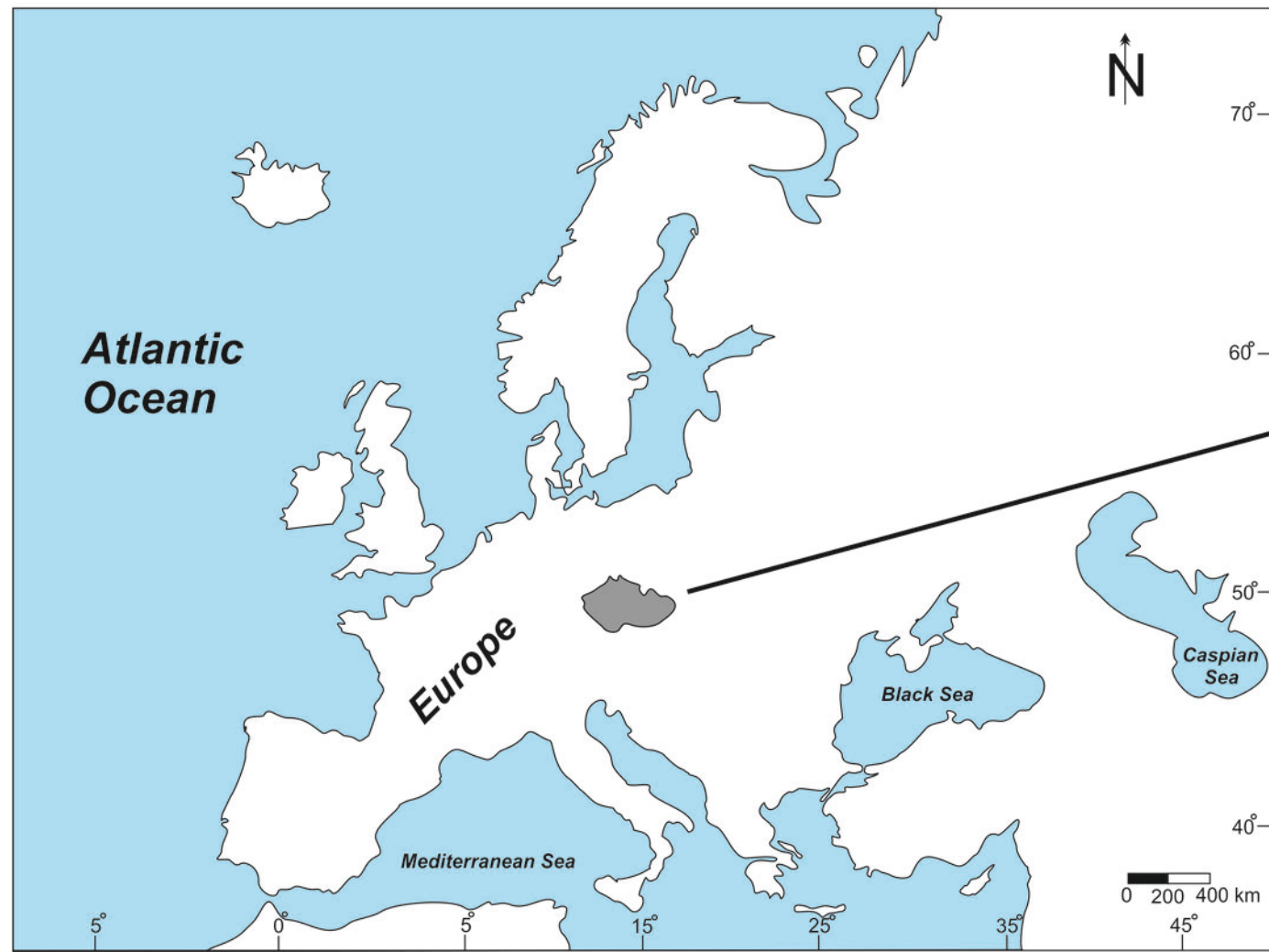
12

13 Sincerely,

14 Hakan Ucar

Figure 1 High quality.

a)



b)



c)

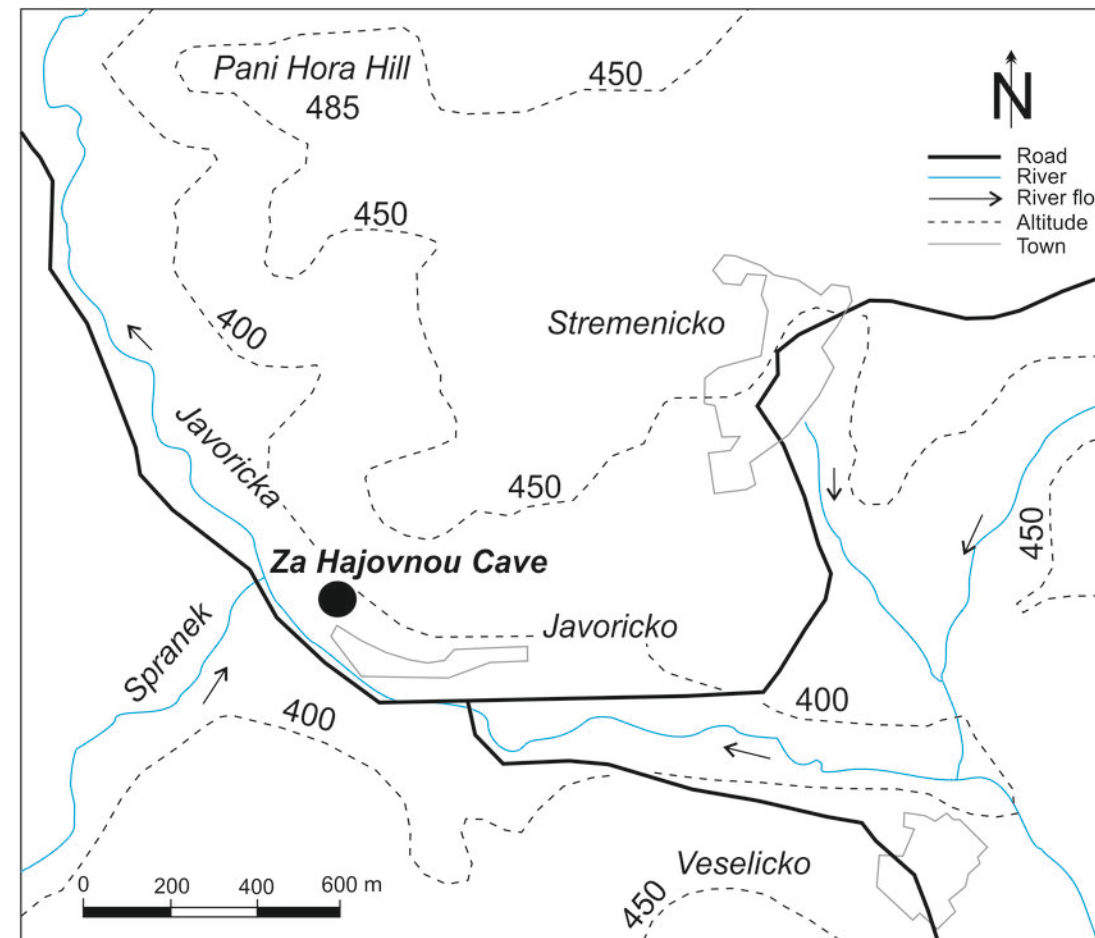
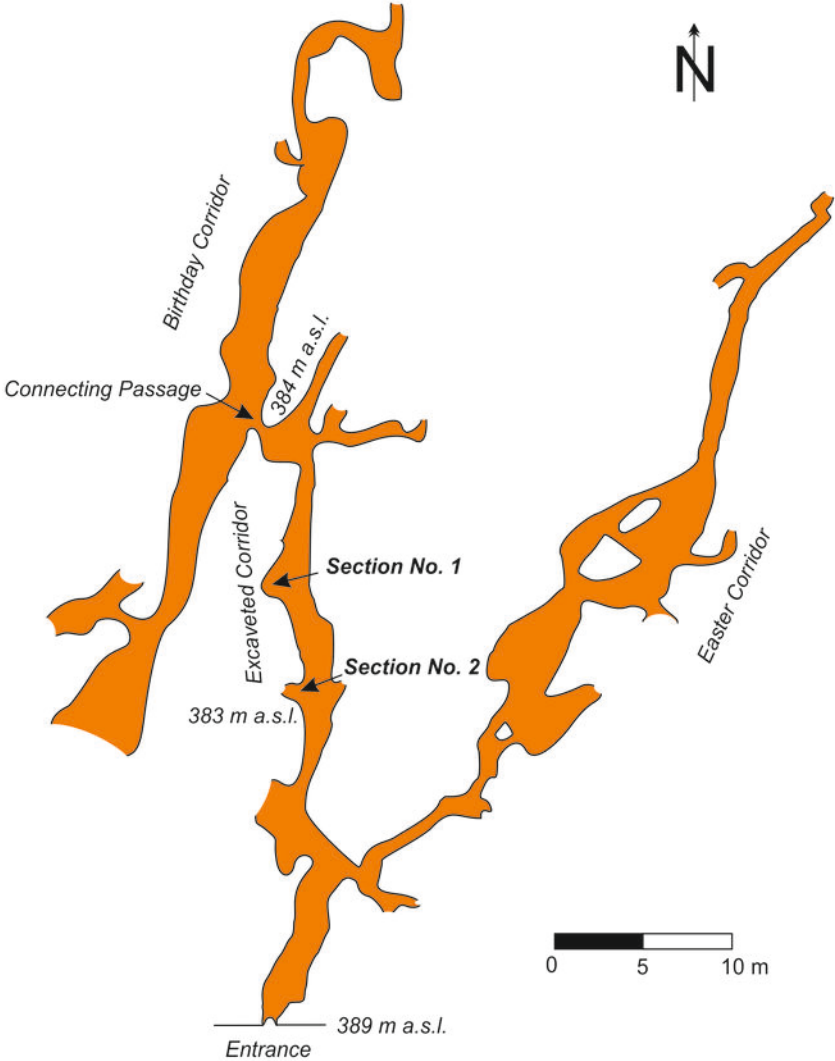


Figure 2 High quality.



Birthday Corridor

Connecting Passage

384 m a.s.l.

Excavated Corridor

Section No. 1

Section No. 2

383 m a.s.l.

Easter Corridor

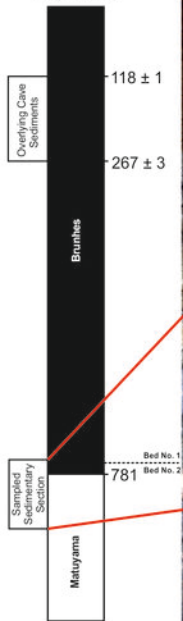


Entrance *389 m a.s.l.*

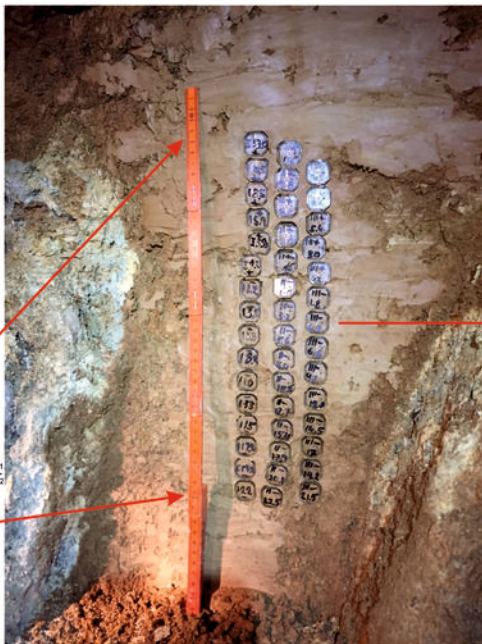
Figure 3 High quality.

a)

Age (ka)



b)



c)

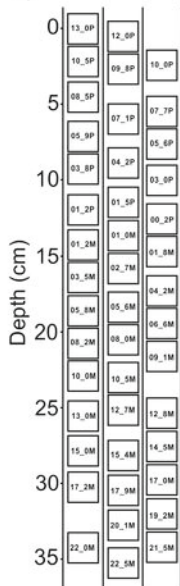
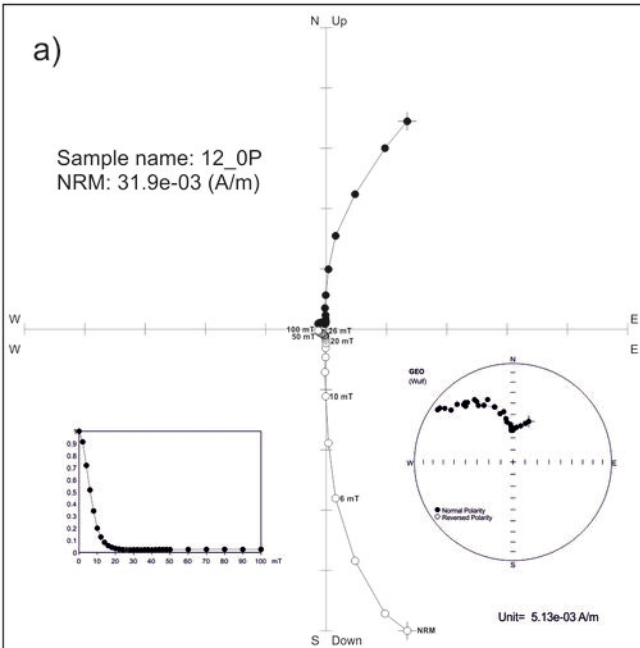


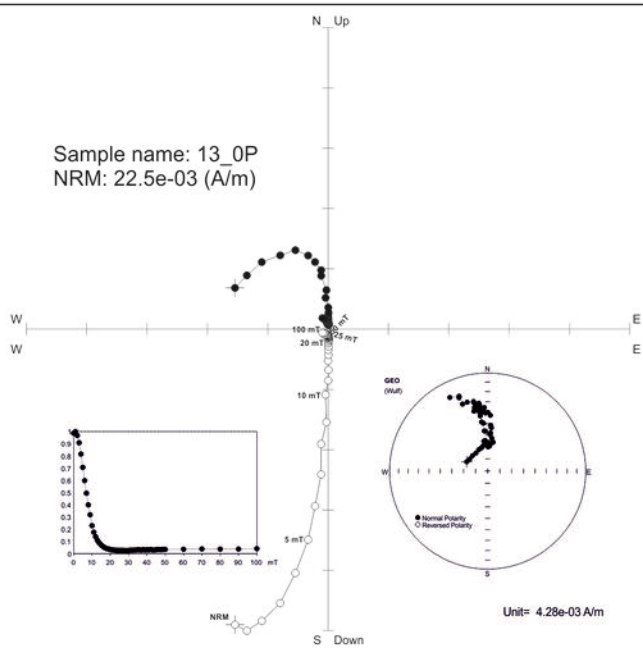
Figure 4 High quality.

a)

Sample name: 12_0P
NRM: 31.9e-03 (A/m)

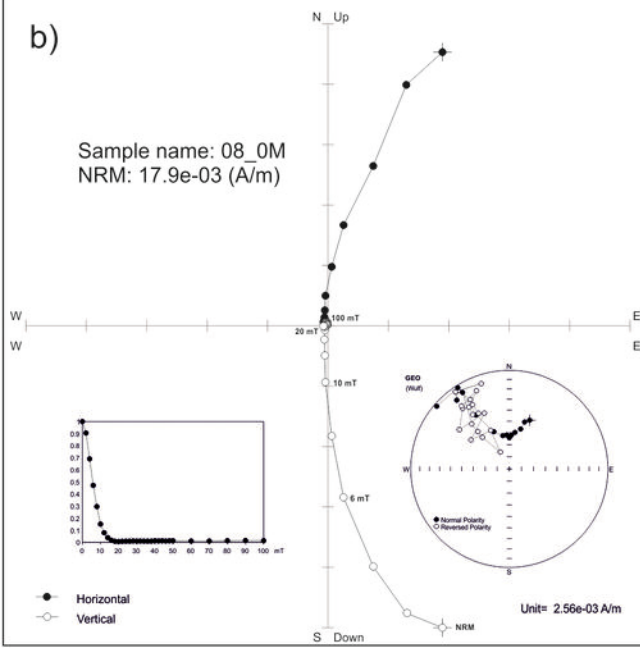


Sample name: 13_0P
NRM: 22.5e-03 (A/m)



b)

Sample name: 08_0M
NRM: 17.9e-03 (A/m)



Sample name: 21_5M
NRM: 8.48e-03 (A/m)

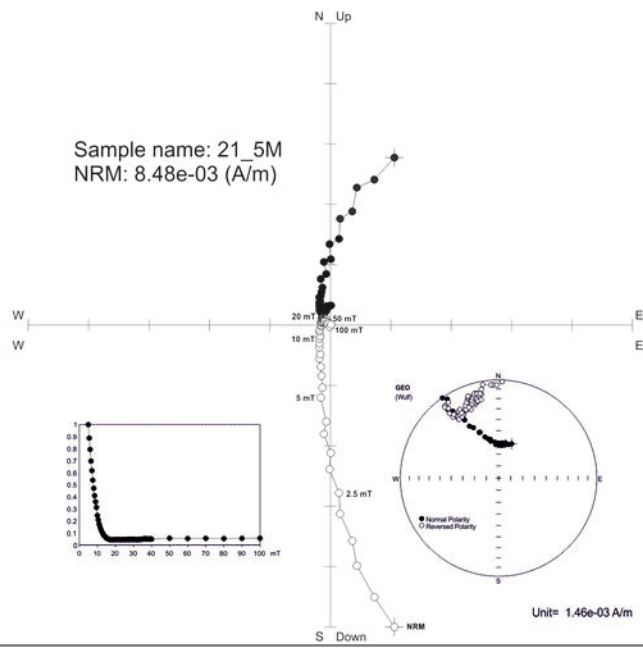


Figure 5 High quality.

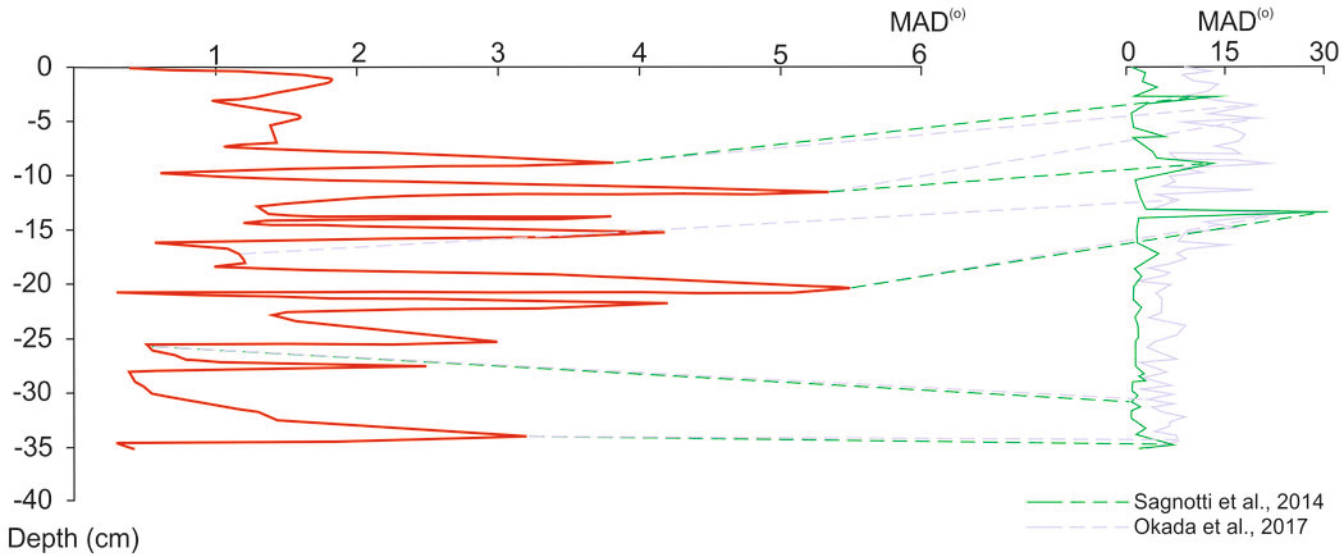


Figure 6 High quality.

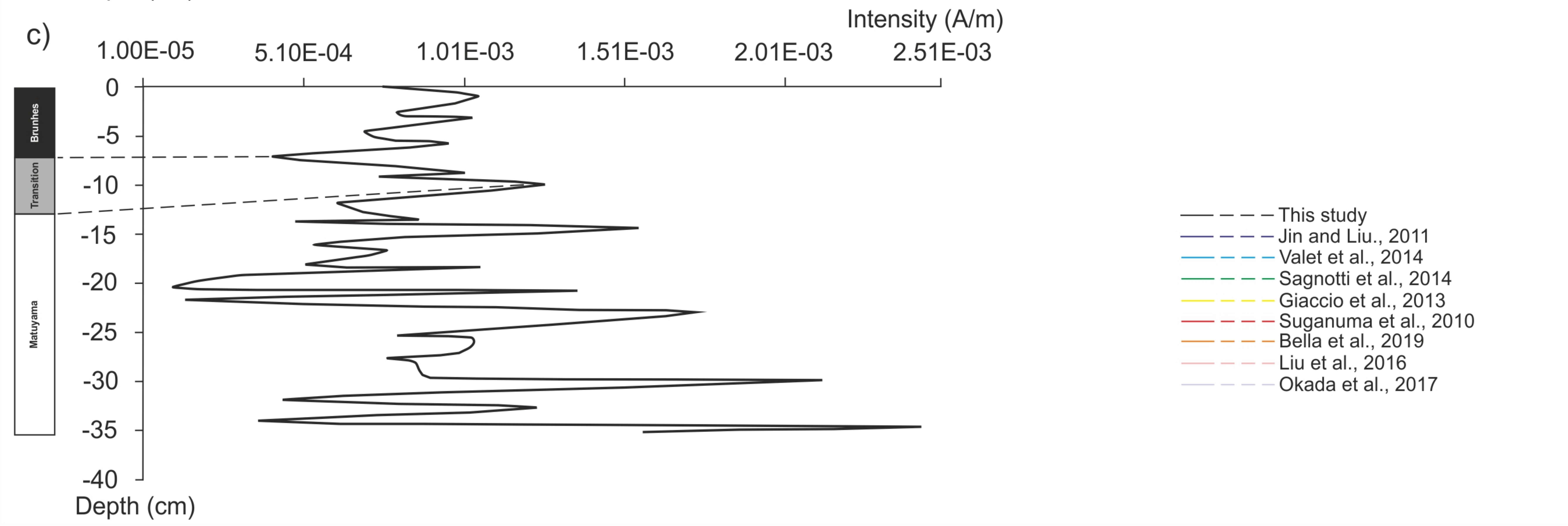
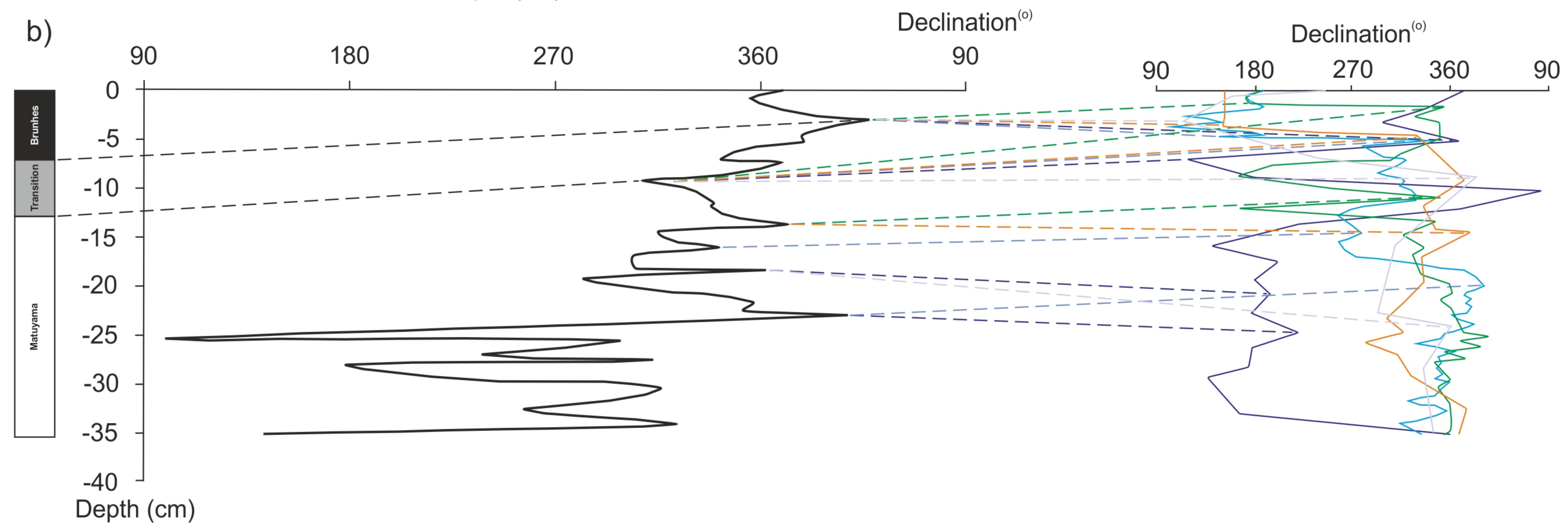
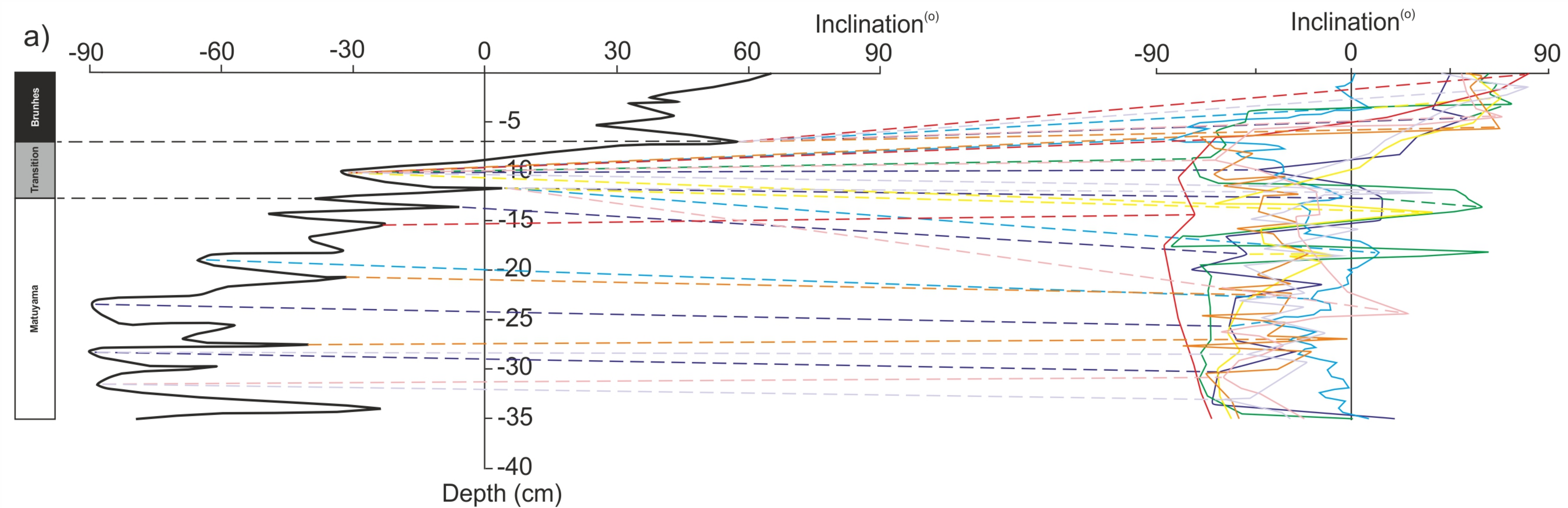
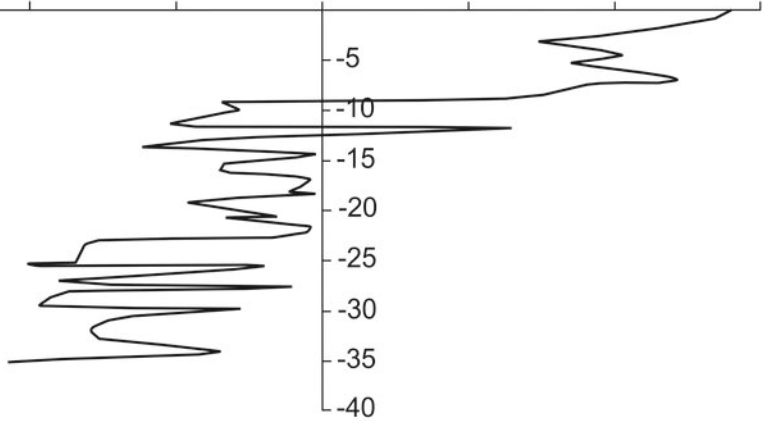


Figure 7 High quality.

VGP latitude^(o)

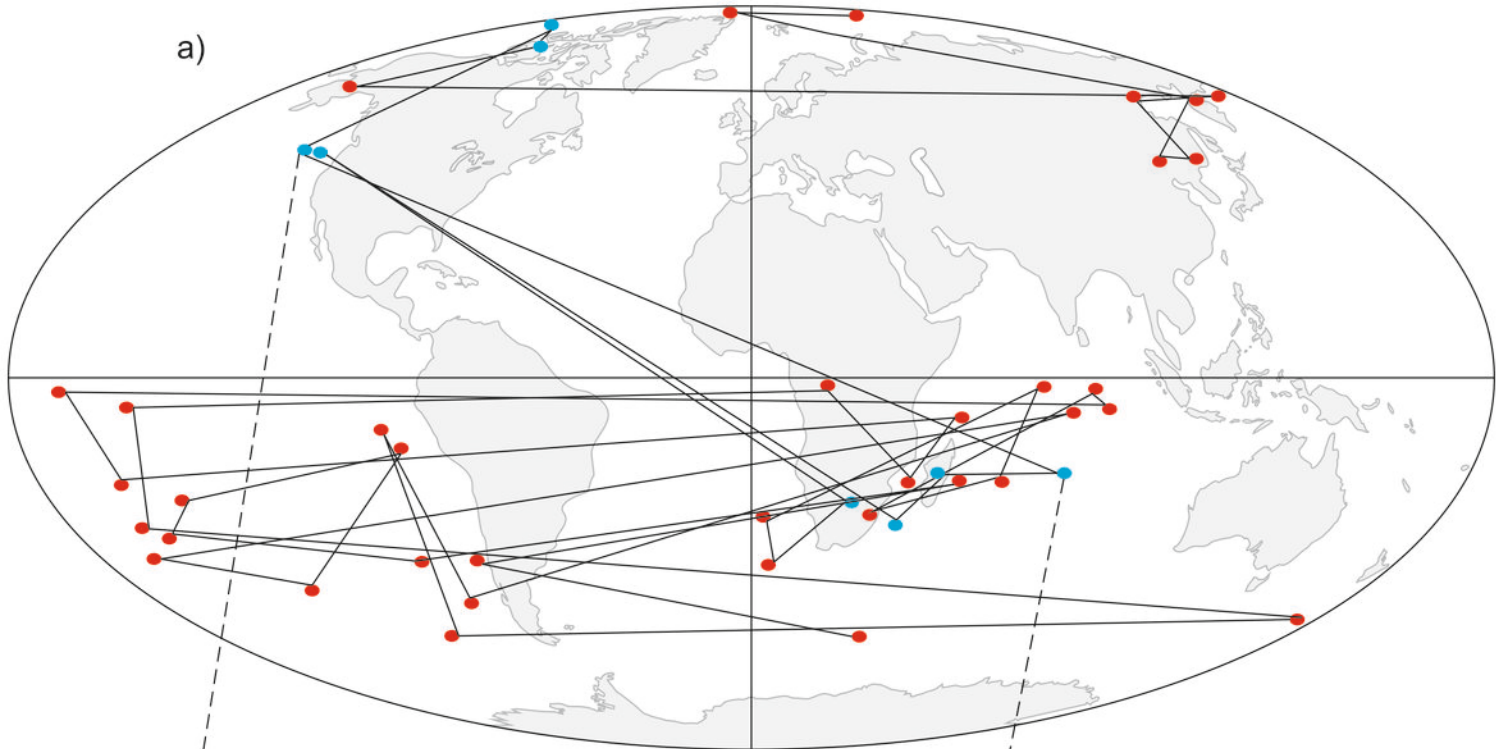
-90 -60 -30 0 30 60 90



Depth (cm)

Figure 8 High quality.

a)



● Normal and Reversed Polarity
● Transition

b)

